

# High-Spatial Resolution Laser Doppler Blood Flow Imaging

Shen Sun <sup>1,\*</sup>, Diwei He <sup>2</sup>, Barrie R Hayes-Gill <sup>3</sup>, Stephen P Morgan <sup>4</sup>

\* Prof. S.P. Morgan: Tel.: ++44 (0)1159 515570

Email: steve.morgan@nottingham.ac.uk

Electrical Systems and Optics Research Division, Faculty of Engineering  
University of Nottingham

**Abstract** A full-field laser Doppler blood flow imaging (LDI) system based on an FPGA (Field Programmable Gate Array) coupled with a high-speed CMOS (Complementary Metal-Oxide-Semiconductor) camera chip has been developed which provides blood flow images with flexible frame rates and spatial resolution. When a high spatial resolution is required, 1280x1024-pixel blood flow images were obtained by processing up to 2048 samples at 0.2 frames per second (fps). Alternatively, a maximum of 15.5fps was achieved by reducing the spatial resolution and sampling points to 256x256 pixels and 128 samples respectively. This system was applied to a high-spatial resolution flow imaging application in which a mixture of water and polystyrene microspheres was pumped through a micropipette (diameter = 250 $\mu$ m) with controlled velocities, and the resulting flow was imaged and processed. The performance was demonstrated by the resulting flow images which are of size 1280x1024 pixels and obtained by processing 2048 samples at each pixel.

**Keywords:** Laser Doppler, Micro Flow, Blood Flow, Microcirculation

## 1. Introduction

In regions of the body where the superficial tissue overlying the blood vessels is relatively thin, the blood vessels and individual red blood cells can be observed. The eye, nailfold, the oesophagus and colon are all examples where high resolution imaging can be performed with significantly reduced effects of light scattering when compared with skin. As full field laser Doppler blood flow imaging (LDI) has been developed, it is becoming a useful tool for imaging the blood flow on the vessels overlaid by a thin superficial tissue. For example LDI has been used in ophthalmology [1-3] to image impairment of tissue blood flow in the pathogenesis of retinal diseases and optic nerve disease. Nevertheless, the small imaging area in the retina requires a high-resolution system including both microscope optics and high-resolution detector arrays, which are challenging for LDI.

We present a LDI system which is characterized by high-spatial resolution (up to 1280x1024 pixels), high number of FFT points

in processing (2048 FFT samples maximum), flexible frame rate (0.2fps ~ 15.5fps) and full field imaging. These features make this system well matched to a high-magnification, high-spatial resolution system such as that used in measuring retinal blood flow. To demonstrate this, the LDI system is coupled with microscope optics (objective lens + eye lens) and applied to imaging flow changes in a micropipette which is a simulation of a retinal capillary of diameter 250 $\mu$ m. Preliminary results show that the resulting resolution is  $\sim 1.2\mu\text{m}/\text{pixel}$  and the flow resolution is at least 0.4mm/s. To the knowledge of the author, this is the first demonstration of high-magnification, high-spatial resolution LDI.

## 2. Experimental Setup

### 2.1 The System

A full-field LDI system is established based on an FPGA platform coupled with a high-speed CMOS camera chip. It can produce up to 1280x1024-pixel blood flow and concentration (*flow/conc*) images constructed by up to 2048 time domain samples at each

pixel. Depending on the resolution and number of samples used for processing, the achieved frame rate ranges from 0.2fps up to 15.5fps which makes the system very flexible.

The system comprises units for imaging, interfacing, storage, processing and control. A schematic of the full-field LDI system is shown in Fig.1.

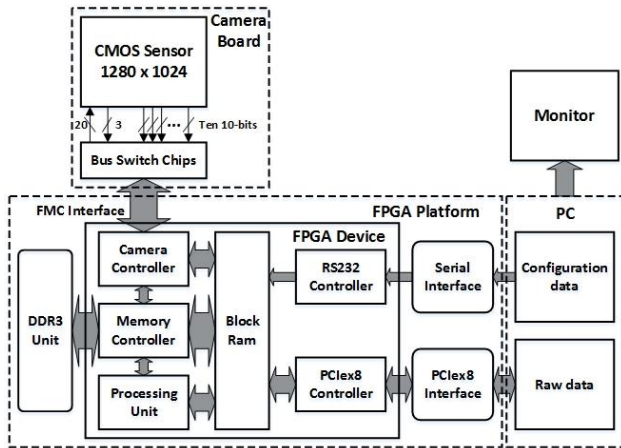


Fig. 1. Schematic of the system showing the main imaging, processing, control and storage units. The CMOS sensor interfaces to the FPGA via the custom-made FMC socket mounted on an 8-layer PCB board (camera board). Various controllers including camera controller, memory controller, RS232 controller and PCIe×8 controller are developed in the FPGA along with the processing unit (processing algorithms) for achieving the functionality. The PC-generated configuration data is sent to the system via the serial interface (RS232). The processed data (blood flow images, blood concentration images, contrast maps and DC images) are transmitted to the PC for further processing and display through the PCIe×8 bus.

A monochrome CMOS sensor (MT9M413, Micron) having 1280H × 1024V 12 μm × 12 μm integrating pixels, 1280 10-bit resolution analogue to digital converters and ten 10-bit-wide digital output ports is driven by an FPGA device (Virtex-6, Xilinx) via a high-speed interface (VITA 57.1 FMC HPC). Due to the large amount of data acquired, a DDR3 SDRAM with capacity of 512 MB is used as internal storage to temporarily store the captured raw data. All controls and processing operations are carried out by the FPGA, and only the processed flow, concentration and averaged DC images are sent to the PC via a PCIe×8 bus.

## 2.2 The Experiment

To simulate blood flow in microcapillaries, polystyrene microspheres (3520A, Duke Scientific, 520nm) were added

to the liquid (distilled water) and pumped to a micropipette (Sigma-Aldrich, Z611239 – 250 EA, internal diameter of 250 μm, external diameter of 860 μm) by a syringe pump (210-CE, Cole Parmer) with controlled velocities. The experimental setup is shown in Fig.2 (a), together with the experimental photograph shown in Fig.2 (b).

A green laser (OXXIUS S.A. 532 S-50-

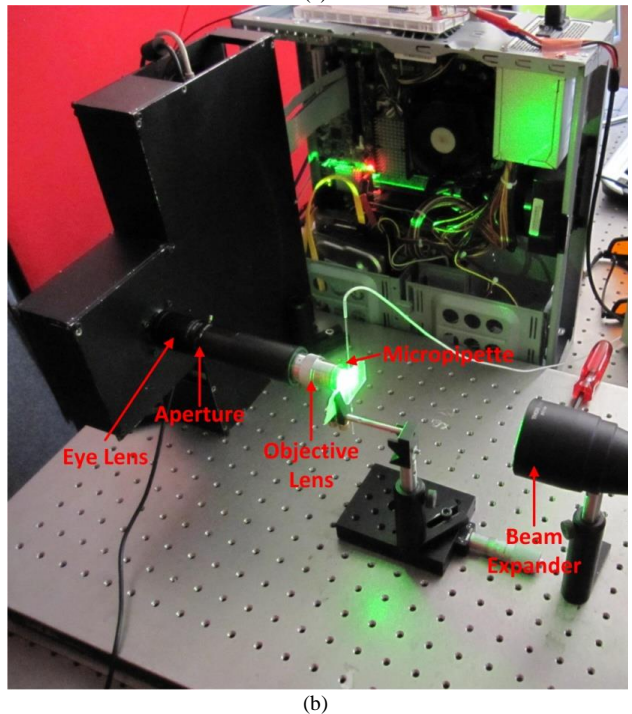
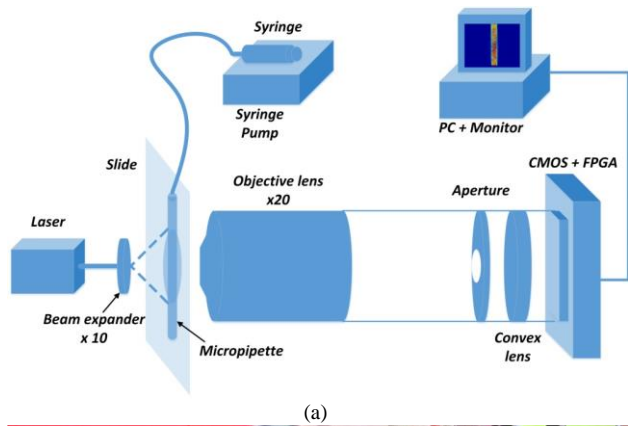


Fig. 2. Experimental setup of high resolution of flow: (a) schematic; and (b) photograph.

COL-PP, 532nm, 50mW) is used as a light source. The laser beam is expanded to a diameter of 9mm by a beam expander (Thorlabs BE10M) and back illuminates the micropipette glued to a microscope slide. A circular field of view (~1.2mm diameter) was imaged by the LDI system through the microscope optical system which consists of a

20x objective lens (MA631, S-Plan 20x, Meiji), an aperture and a convex lens ( $f = 25.4\text{mm}$ ). The FPGA-processed flow images were constructed by 2048 1280x1024-pixel samples and sent to a general purpose PC for further processing and display. Images were recorded over a range of velocities from 0mm/s to 16mm/s in increments of 0.4mm/s.

The optical path of the microscope optic is indicated in Fig.3. The object (micropipette) is positioned 3mm away from the objective lens through which a 20 times magnified image of the object is formed on the intermediate image plane having a distance of 60mm to the objective lens. The intermediate image is

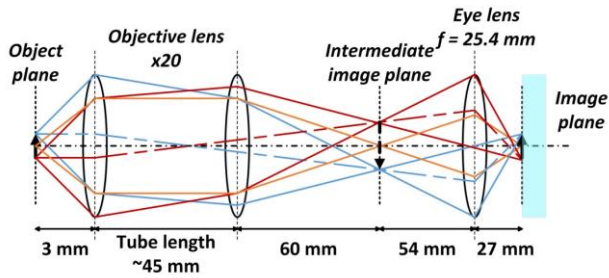


Fig. 3. Optical path of the microscope optic. The magnifications of the objective lens and the eye lens are x20 and x0.5 respectively. The magnification of the microscope optic is x10.

imaged onto the CMOS sensor via the eye lens ( $f = 25.4\text{mm}$ ) standing 27mm away from the CMOS sensor and 54mm away from the intermediate image plane, with a magnification of 0.5. With this optical configuration, the magnification of the microscope system is, therefore, 10. As the pixel size is  $12\mu\text{m}$  by  $12\mu\text{m}$ , the resolution of the system is  $1.2\mu\text{m}/\text{pixel}$ .

### 3. Result

The liquid (microspheres + water) flowing in the micropipette at various speeds was imaged by  $1280 \times 1024$  pixels, which is shown in Fig.4.

As can be seen, the imaged field is a circular area which is approximately 1000 pixels in diameter. Since the magnification of the microscope optic is 10, the imaging area is of diameter 1.2mm (pixel size is  $12\mu\text{m}$  by  $12\mu\text{m}$ ). The micropipette channel is vertically displayed on the image and occupies about 200 pixels horizontally, corresponding to a

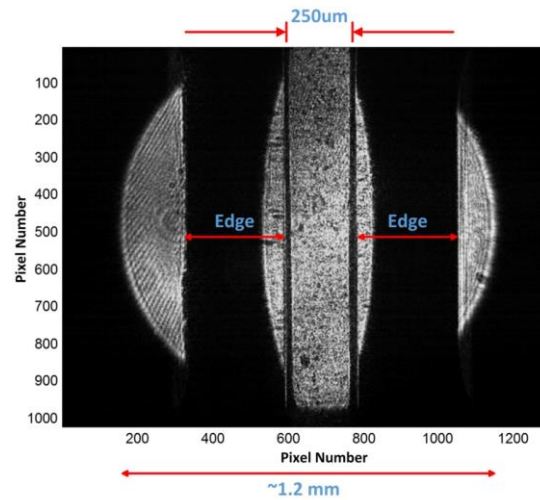


Fig. 4. Raw DC image of the liquid flowing in the micropipette. The micropipette is  $250\mu\text{m}$  in internal diameter and the imaging area is of diameter  $\sim 1.2\text{mm}$ .

diameter of  $250\mu\text{m}$ . The two dark areas in the image field and the semicircle areas adjacent to the  $250\mu\text{m}$  channel (the light reflected from the edge of the internal layer) are due to the static external part of the micropipette.

The flow rate began from 0mm/s (Brownian motion) and rose up to 16.0mm/s with a fixed incremental step of 0.4mm/s. Each flow image was processed by 2048 samples and refreshed at a rate of 0.2fps. A typical flow image obtained at a rate of 6.4mm/s is shown in Fig.5. Flow changes with the increasing speed are indicated by the flow images displayed in Fig.6.

Obviously, except the micropipette there is no flow presented on the images, and the measured flow increases as the flow rate increases. Therefore, the high-resolution LDI system is capable of detecting the flow changes. It is interesting to note that the image is immune to the DC light and external diameter of the tube since there is no flow presented although they are clearly displayed in the raw DC image (Fig.4). This indicates that the system is likely to be immune to surface reflections which are a recognized problem in imaging the microcirculation [4, 5].

Averaging the flow values of a  $640 \times 160$ -pixel area on the micropipette as marked in

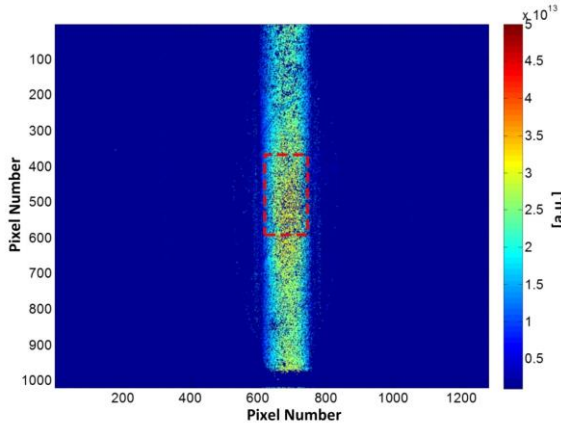


Fig. 5. A typical flow image obtained at 6.4mm/s flow rate. The visible flow area is of size  $\sim 200 \times 1,000$  pixels corresponding to  $250 \mu\text{m} \times 1,200 \mu\text{m}$  internal channel of the micropipette.

Fig.5, the flow profile (flow plotted against the actual speed) is shown in Fig.7.

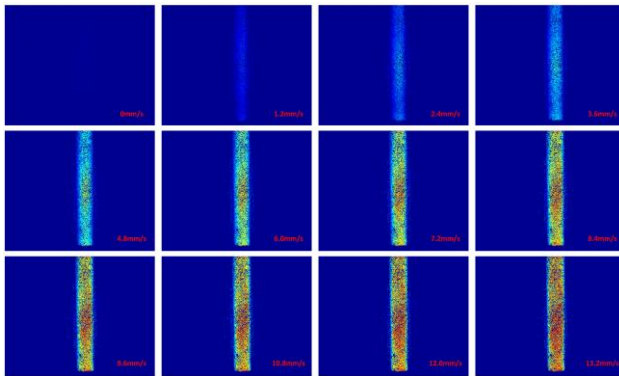


Fig. 6. Flow images obtained at flow rates of 0mm/s, 1.2mm/s, 2.4mm/s, 3.6mm/s, 4.8mm/s, 6.0mm/s, 7.2mm/s, 8.4mm/s, 9.6mm/s, 10.8mm/s, 12.0mm/s and 13.2mm/s, the flow rate is increased from left to right and top to bottom, the scale range for display is fixed at  $1e12 \sim 5e13$

From Fig.7, it is clear that the measured flow linearly rises as the actual speed increases until it approaches  $\sim 8\text{mm/s}$  after which the flow slightly and nonlinearly increases with flow rate (the flow rate starts to saturate). The reason is that aliasing occurs when the beat frequency of LDBF signals is beyond the bandwidth of the LDI system which is from 250Hz to 7,350Hz.

It also can be noted that small changes of speed (0.4mm/s) can be measured by the high-resolution LDI system when it occurs in the detectable speed range (0mm/s – 8mm/s). The

error defined as the standard deviation of mean flow gradually increases with flow speed and reaches a maximum when the flow speed exceeds the detectable range.

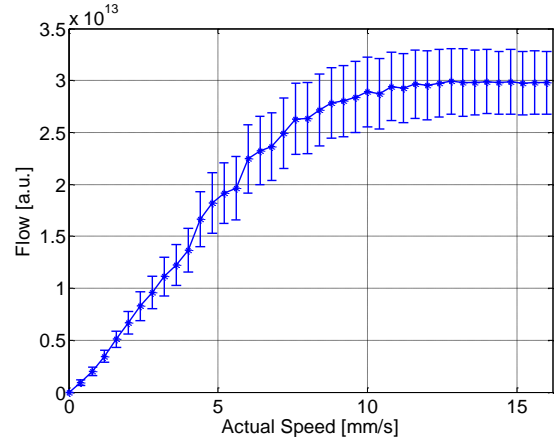


Fig. 7. Flow profile, flow value plotted against actual speed. The error bar is defined as the standard deviation of the flow values of all pixels in the selected region. Limited by the system bandwidth (250Hz  $\sim$  7,350Hz), the flow with velocity higher than 8mm/s is unable to be correctly measured.

In order to quantitatively evaluate the accuracy of measurement, the parameter, relative flow, which is the baseline-calibrated flow (Eq.1), is adopted for indicating flow changes. The relative flow responding to the relative speed (speed changes, Eq.2) is plotted in Fig.8, together with the theoretical line.

$$\text{Relative flow} = \frac{\text{flow}}{\text{baseline flow}}, (1)$$

$$\text{Relative speed change} = \frac{\text{speed}}{\text{baseline speed}}, (2)$$

The relative flow is comparable with the ideal value in the linear region corresponding to the detectable range of flow rate. The mean relative error which is defined as Eq.3 is 7.7%.

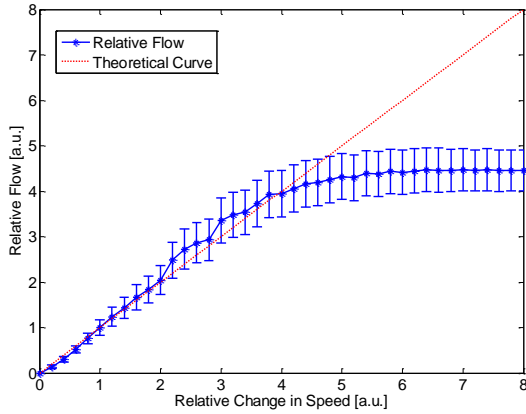


Fig. 8. Relative flow plotted against the relative changes in speed. The baseline is at a flow speed of 2mm/sec. The dashed line is the plot of the theoretical relative flow against the relative changes in speed. The error bar of the relative flow is defined as the standard deviation of the relative flow values of all pixels in the selected region.

**Relative Error**

$$= \frac{|Theoretical\ Flow - Relative\ Flow|}{Theoretical\ Flow} \times 100\% \quad (3)$$

It can be concluded that the proposed high-resolution LDI system is capable of accurately (less than 0.1 relative errors) measuring flow changes in the 250µm micropipette when the absolute flow speed is less than 8mm/s.

**4. Conclusion**

The full field LDI system has been demonstrated for high spatial resolution of flow. In conjunction with a microscope optical system, high-resolution flow imaging (1.2 µm/pixel , 1280x1024 pixels) was achieved with an accuracy of <10% relative errors. In the detectable range (0mm/s ~ 8mm/s), the system is capable of linearly measuring at least 0.4mm/s changes in flow rate, which means the system is sensitive to flow.

As the high cut-off frequency of the

system bandwidth is 7,350Hz, the detectable flow rate is limited to be no more than 8mm/s (as shown in Fig.7) over which the flow rate cannot be correctly measured. However, it is feasible to measure higher flow rates by extending the system bandwidth with the use of smaller ROIs (region of interest) or faster cameras.

**5. Reference**

[1]. Kimura, I., Shinoda, K., Tanino, T., Ohtake, Y., Mashima, Y., and Oguchi, Y., (2003), *Scanning laser Doppler flowmeter study of retinal blood flow in macular area of healthy volunteers*, Br J Ophthalmol., 87.12 (2003): 1469-1473.

[2]. GT, FEKE., (2006), *Laser Doppler instrumentation for the measurement of retinal blood flow: theory and practice*, Bull. Soc. Belge Ophtalmol, 302 (2006): 171-184.

[3]. Forst, T., Weber, M.M., Mitry, M., Schondorf, T., Forst, S., Tanis, M., Pftzner, A., and Michelson, G., (2012), *Pilot Study for the Evaluation of Morphological and Functional Changes in Retinal Blood Flow in Patients with Insulin Resistance and/or Type 2 Diabetes Mellitus*, Journal of Diabetes Science and Technology, 6.1. (2012): 163-163.

[4]. Ince, C., (2005), *Sidestream dark field imaging: an improved technique to observe sublingual microcirculation*, Crit Care, 9.Suppl 1 (2005): P72.

[5]. van Beers, E., Goedhart, P., Unger, M., Biemond, B., and Ince, C., (2008), *Normal sublingual microcirculation during painful crisis in sickle cell disease*, Microvas Res, 76.1 (2008): 57-60.